n y n

School of Mathematical and Physical Sciences

A c An n
n n n n n y
n n

n c

August 2010

This dissertation is a joint MSc in the Departments of Mathematics and Meteorology and is submitted in partial fulfilment of the requirements for the degree of Master of Science

Ac n n

I acknowledge the modelling groups, the Program for Climate Model Diagnosis and Intercomparison (PCMDI) and the World Climate Research Programme's (WCRP's) Working Group on Coupled Modelling (WGCM) for their roles in making available the WCRP CMIP3 multi-model dataset. Support of this dataset is provided by the Office of Science, U.S. Department of Energy.

20th Century Reanalysis data is provided by the NOAA/OAR/ESRL PSD, Boulder, Colorado, USA, from their website at http://www.esrl.noaa.gov/psd/

Support for the Twentieth Century Reanalysis Project dataset is provided by the U.S. Department of Energy, Office of Science Innovative and Novel Computational Impact on Theory and Experiment (DOE INCITE) program, and Office of Biological and Environmental Research (BER), and by the National Oceanic and Atmospheric Administration Climate Program Office.

I would very much like to thank the Natural Environment Research Council (NERC) for funding my MSc with an NERC Studentship, all the teamakers who's wonderful products have fuelled ideas throughout this project, and last, but not least, my supervisor: Valerio Lucarini. Mille grazie!

c n

I confirm that this is my own work and the use of all material from other sources has been properly and fully acknowledged

Signed:...

Simon Driscoll

n n

L

n c n

There are only a few atmospheric variables that can be used to effectively compare the large scale circulation of the true observed atmosphere and the simulated atmosphere in climate models. Angular Momentum, a fundamental quantity of central importance to the atmosphere, and indeed any rotating system (as mentioned in Egger et al. (2007)), is one of these. The Angular Momentum budget represents a beautiful example of how the atmosphere, oceans and solid earth interact and are inextricably linked through a conservation law (Oort (1989)), and it is of interest to researchers studying any one of these different elements.

Lucarini (2008) points to the need for further confirmation of the basic physical and dynamical processes in climate models, and Peixoto and Oort (2007) note that applying the theory of angular momentum to the climate system can lead to general conclusions about the climate system, which we can use to test both the observed values of the real atmosphere and that of climate models, individually, and in comparisons.

The total angular momentum of the atmosphere, oceans and earth does not change except for a slow secular decrease due to the gravitational force exerted by planets. However, there is transfer between the three components of the earth mentioned above, and if angular momentum increases in the atmosphere it must have been transferred from one of the other elements into the atmosphere, analogously if the atmosphere loses angular momentum it needs to transferred to one of these elements.

In this dissertation we are concerned with the theory of angular momentum in the earth's atmosphere and the torques (the 'turning' or rotational forces) that affect the angular momentum of the atmosphere, and whether the what we discern from the theory can be seen in what is called a 'reanalysis observation dataset' and three state of the art climate models. Reanalysis observation datasets are a literally a re-analyses intended to replace the original analyses observation datasets (literally the recorded quantities of atmospheric variables) because of the need to alleviate many problems that arose from

momentum it does not mean that it is realistic and giving accurate values of the atmospheric variables. A reanalysis dataset or climate model may be physically internally consistent and conserve angular momentum but not actually be realistic: for example, it may consistently under or over estimates the sizes of events, or for how long they last and when they occur. This noted, physical consistency is still something we want to hope for for good models.

we can also look in passing for evidence of model ‘drift’ (dri

An n n

y

An n

Before we consider Angular Momentum of the Earth's Atmosphere we shall consider *linear* momentum. The Linear Momentum, p

$$\mathbf{m} = \rho \mathbf{r} \times (\mathbf{u}_{\mathbf{rel}} + \mathbf{\Omega} \times \mathbf{r}) \qquad (2.8)$$

where ρ is the density of the air parcel. Therefore the total Angular Momentum of the Earth's Atmosphere, again a vector, is

$$\mathbf{M} = \int_v \rho \mathbf{L} dV = \int_v \int_v \rho \mathbf{r} \times (\mathbf{u}_{\mathbf{rel}} + \mathbf{\Omega} \times \mathbf{r}) dV \qquad (2.9)$$

where v is the volume of the atmosphere.

One can also split the Earth's Angular Momentum $\mathbf{M}$, aswell as the velocity, into two conceptually useful parts: the 'mass' part of angular momentum, $\mathbf{M}_{\Omega}$, and the 'relative' part $\mathbf{M}_{\mathbf{r}}$. The mass part of the Earth's Angular Momentum is the amount of angular momentum the atmosphere would have if all the atmosphere were at rest vertically and

51(r)-0.2Ω1061(m)horizontally, staying at [illegible]

Egger et al. (2007).

Therefore velocity can be written as:

$$\mathbf{v} = u\mathbf{e}_\lambda + v\mathbf{e}_\theta + w\mathbf{e}_r \tag{2.11}$$

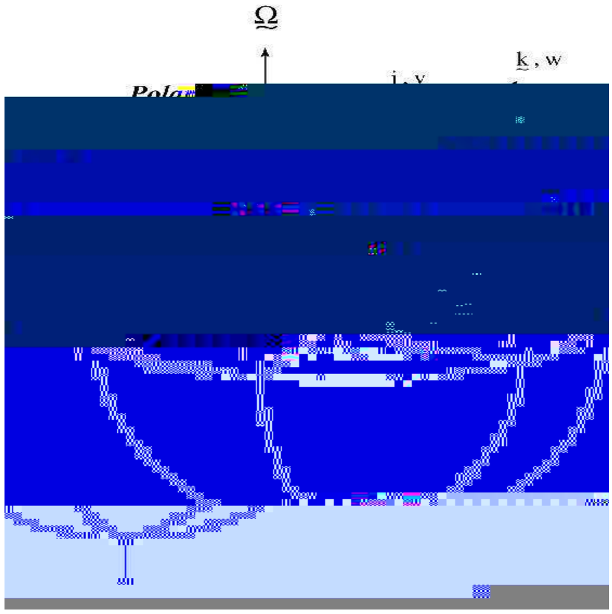

Figure 2.1: Rotating Coordinate System

In this project we will look at the total axial component of atmospheric angular momentum M_3, given by

$$M_3 = \int_V m_3 dV = \int_V \rho(u + \Omega r\cos\theta) r\cos\theta dV \tag{2.12}$$

which can be seen from equation (2.9), recall the definitions from section 2.3, and note that ‘u’ is the east-west component of the wind velocity (where a wind moving towards the east is taken as positive, and a wind moving towards the west is taken as negative). We

where u_n is the normal outward component of v across the surface S of the volume v. Note, at φ_1 this outward normal across the surface points towards the south pole, and at φ_2 this outward normal points towards the north pole. The first term on the right hand side corresponds to the flux of angular momentum across these vertical boundaries, whilst the next two terms correspond to the flux of angular momentum across the earth's surface, these fluxes are illustrated in figure 2.2. The physi


n

and therefore, as p

called the mountain torque, which we now define as T_M. This is the torque that occurs due to the pressure exerted on any raised surface (and importantly pressure exerted on mountains), and that Γ is what is called the friction torque, T_F, which is the torque from the friction applied by the atmosphere to the surface of the earth. Thus (2.27) becomes

$$\frac{dM}{dt} = T_M + T_F \tag{2.28}$$

It is important to note, that throughout this project we take, in line with convention, that a torque that increases the angular momentum of the atmosphere to be a positive torque, and one that decreases the angular momentum of the earth to be a negative one.

Although equation (2.28) holds true analytically, when we work on numerical models we need to add another torque. This torque, called the gravity wave torque, is the part of the mountain and friction torque too small to be resolved on a numerical grid, we shall discuss this in more detail in 2.8. Thus for numerical models a form equivalent to (2.28) may be given where, on the right hand side, the gravity wave torque is included, so that we have

$$\frac{dM}{dt} = T_M + T_F + T_G \tag{2.29}$$

Of course this means

$$M(t) - M(0) = \int_0^t T_F + T_M + T_G \, dt \tag{2.30}$$

and it is interesting to note that equation (2.26) implies that over long periods of time the total torque time average over a long period of time is zero i.e. there is no change in the angular momentum of the atmosphere over long periods of time.

We shall now summarise the main torques.

c n

The friction torque is the torque that is exerted on the earth's surface due to the frictional force that occurs because of the wind directly above the Earth's surface moving relative to the solid earth. If there is an net global westerly surface wind (i.e. a surface wind *from* the west) the atmosphere will speed the earth's rotation up, transfer angular momentum to the earth, and thus the atmosphere loses angular momentum. Analogously, if there is a net easterly surface wind (i.e. a surface wind *from* the east), the atmosphere slows down the rotation of the earth and angular momentum is transferred from the earth to the atmosphere. The Friction Torque is given by

$$T_F = R^3 \int_{\lambda=0}^{2\pi} \int_{\theta=-\pi/2}^{\pi/2} \tau_f \cos^2\theta \, d\theta \, d\lambda \qquad (2.31)$$

where τ_F is the average east-west surface friction stress per unit area, and R is the average radius of the earth from its centre.

Mountain Torque is a function of pressure and orography and is the 'turning force' exerted this scale, it is quite hard to separate what is the friction torque and what is mountain torque in a model, and this is why we said the gravity wave torque was the part of the mountain and friction torque too small to be resolved.

The gravity wave torque is given by

$$T_G = R^3 \int_{\lambda=0}^{2\pi} \int_{\theta=-\pi/2}^{\pi/2} \tau_g \cos^2\theta \, d\theta \, d\lambda \tag{2.34}$$

where τ_G is the average east-west surface gravity wave stress per unit area.

There are numerous Torques that act to change the Angular Momentum of the Atmosphere, however they are a lot smaller than mountain, friction and gravity wave torques, and did not appear in the above derivation because we ruled the corresponding terms at the start of our derivation. A comprehensive discussion of things that can produce torques is given in Weickmann and Sardeshmukh (1994), we very briefly mention a few of these 'other' torques.

There are torques from *outside* the earth-atmosphere-ocean (EAO) system, such as solar winds, electromagnetic forces, and a tidal torque exerted by the moon and other planets on the Earth that causes a slow secular decrease in the angular momentum, this corresponds to a loss rotation of about 2 ms/century, Peixoto and Oort (2007).

There are also a number of other Torques coming from within the EAO system such as the Moisture or Precipitation Torque and the Ocean or Continent Torque. However the contributions from all these torques are negligible in comparison to the mountain, friction and gravity wave torque, as mentioned in Peixoto and Oort (2007) and Egger et al.(2007). For the angular momentum budget of the atmosphere the friction and mountain torques are both essential, and this has long been realised, e.g. White (1949).

$$\frac{1}{2\pi}\int_0^{2\pi} A(\lambda,\theta)d\lambda \tag{3.1}$$

is plotted($\forall\theta$). Note the whole term in (3.1) is commonly defined as $[A(\theta)]$. In agreement with our general wind pattern discussed above we see that, on average the Friction Torque is positive in areas where the average wind direction is West to East, and negative where the average wind direction is West to East. In weather and climate studies Torques are generally given in the unit Hadleys or 'Had', where 1 Had = 10^{18}kg m^{2}s^{-2}. The values in the graph, a discretized form of (3.1), are given not $\forall\theta$ but for latitude strips, which is why we see the units are Hadleys per degree.

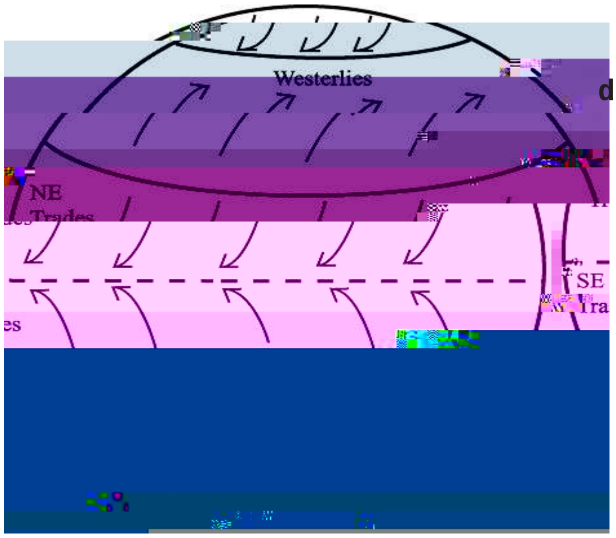

dntar3)9.0492351()8.05031(e)9.0492351(

Figure 3.1: Prevailing Surface Winds

The Himalayas and the Rocky Mountains have been shown to be big contrubutors to mountain torque activity as mentioned in Weickmann et al. (2007). At the Himalayas and the Rocky Mountains generally Angular Momentum is lost a

Figure 3.2: Friction Torque Latitudinal Profile. A zonal average of T_F over June 1987-May 1988, from Madden and Speth (1995).

y

We could not find a latitudinal profile for the gravity wave torque, however there is little doubt that the magnitude of the gravity wave torque, simply because it is the unresolved part of the mountain and friction torque, will be large around the the major mountain ranges i.e. the rocky mountains and the himalayas.

An n n

We are now able to draw a rough picture: Angular Momentum enters the Atmosphere through Friction Torque around the Equator and then the Friction Torque at the midlatitudes and the Mountain Torque and mainly the Himalayas and Rocky Mountain Ranges sap the atmosphere's angular momentum.

Because Angular Momentum is sent into the the Earth at midlatitudes (a sink for the atmosphere) and a source for the atmosphere is the 'excess' angular momentum that comes out of the Earth at the equator there must be a flow of angular momentum from the equator to the midlatitudes through the atmosphere and a flow from the midlatitudes to the equator in the oceans or the solid Earth.

Poleward movement of angular momentum occurs through either the movement of mass in the atmosphere or midlatitude waves or Eddies. The significance of the midlatitude waves or eddies to the poleward contribution of angular momentum was shown by Victor

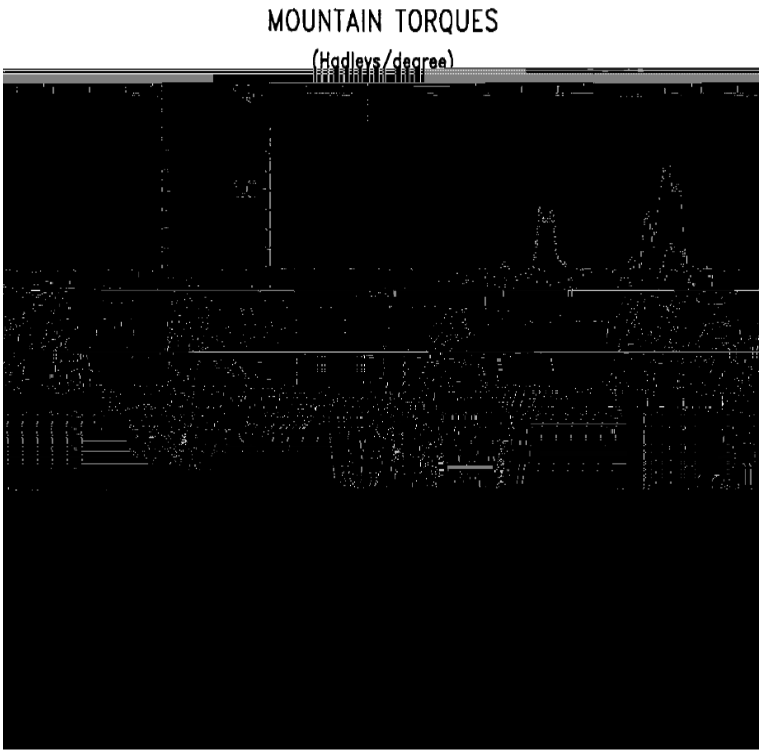

Figure 3.3: Mountain Torque Latitudinal Profile. A zonal average of T_M over June 1987-May 1988, from Madden and Speth (1995).

Starr, as mentioned in Oort (1989).

The right hand side of figure 3.4 shows the streamlines of angular momentum through the atmosphere, where ψ_M is the flux of angular momentum (the left s 630099(d)0332.695(1)0.622099(d)03

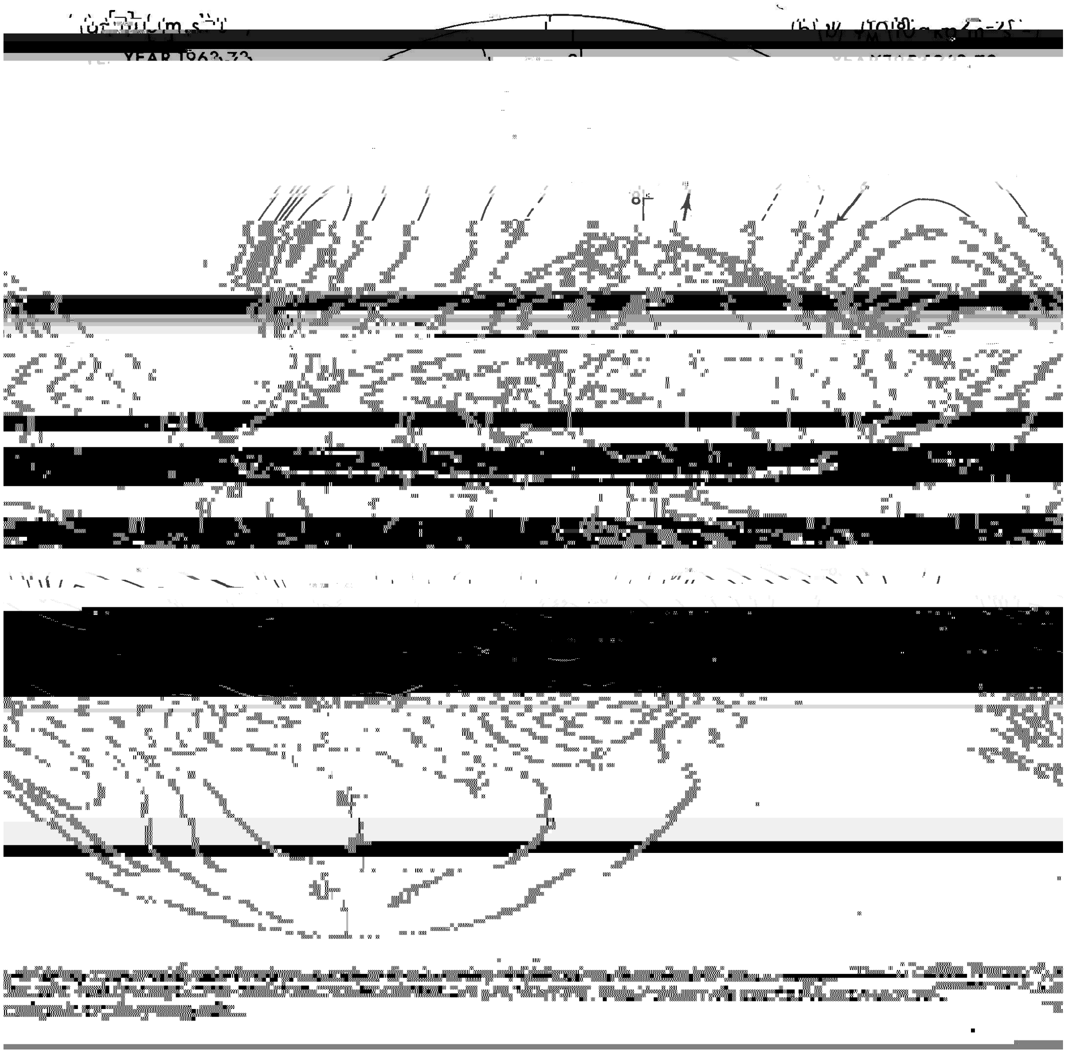

Figure 3.4: Cross sections of the mean zonal flow in ms^{-1} on the left hand side of the earth

n n n L n y n A c An

The angular momentum of the atmosphere increases and decreases in an annual cycle due to the seasons. The angular momentum of the atmosphere is at its largest in the northern hemisphere winter, and is at its minimum in the northern hemisphere summer due to,

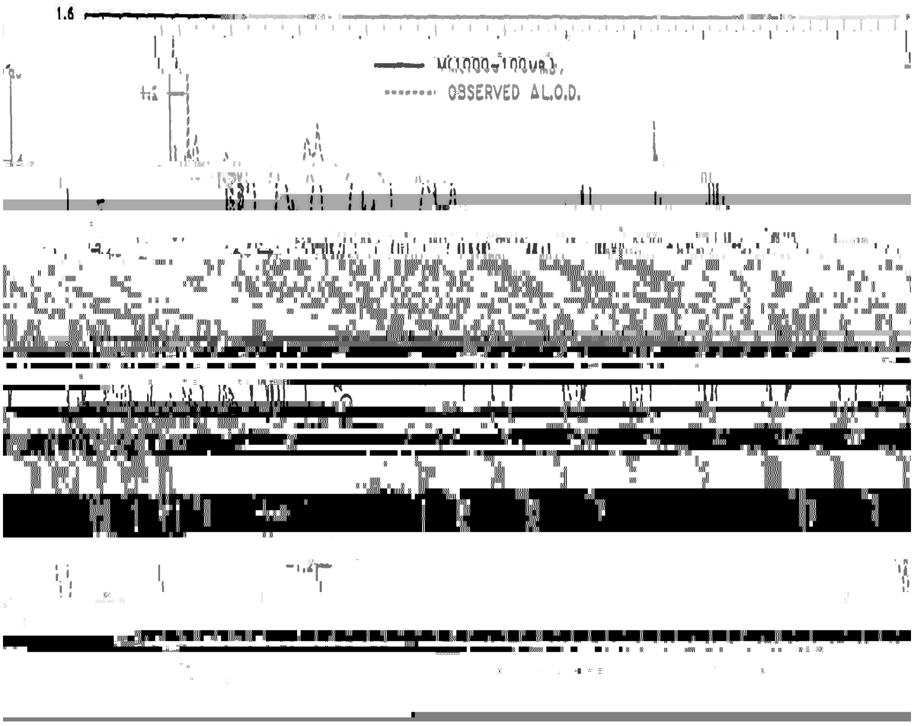

Figure 3.5: LOD and Relative Angular Momene,1(r)5Rf1(u)0572898(r)-00368804(o)0.0492351(r)-3232(F

$$\frac{\Omega \Delta T}{T} = -\frac{\Delta M_{Rel}}{I_e} \tag{3.7}$$

Defining $\Delta T = \Delta LOD$, and using $I_e \approx 7.04 \times 10^{37}$kg m^2 the change in the length of day then can be given (see Rosen et al. 1987) by the following formula:

$$\Delta LOD = 0.168 \Delta M_{Rel} \tag{3.8}$$

where ΔLOD is in units of milliseconds (ms) and ΔM_{Rel} is in units of 10^{25}kg m^{2}s^{-1}. This yields approximately a 0.8 ms increase in the LOD at July than the LOD in January and this corresponds to a 2ms^{-1} change in zonal wind.

There have been debates about the value for the momentum of inertia of the solid earth in this calculation. The solid earth is composed of many different layers, but may be grouped into three main layers, and from inside to outside they are: the core, the mantle and the crust. Debates are present as to whether the mantle and crust may be rotating at a different rate to the liquid core, and as noted by Peixoto and Oort (2007) this is the reason for why the moment of inertia was chosen as 7.04

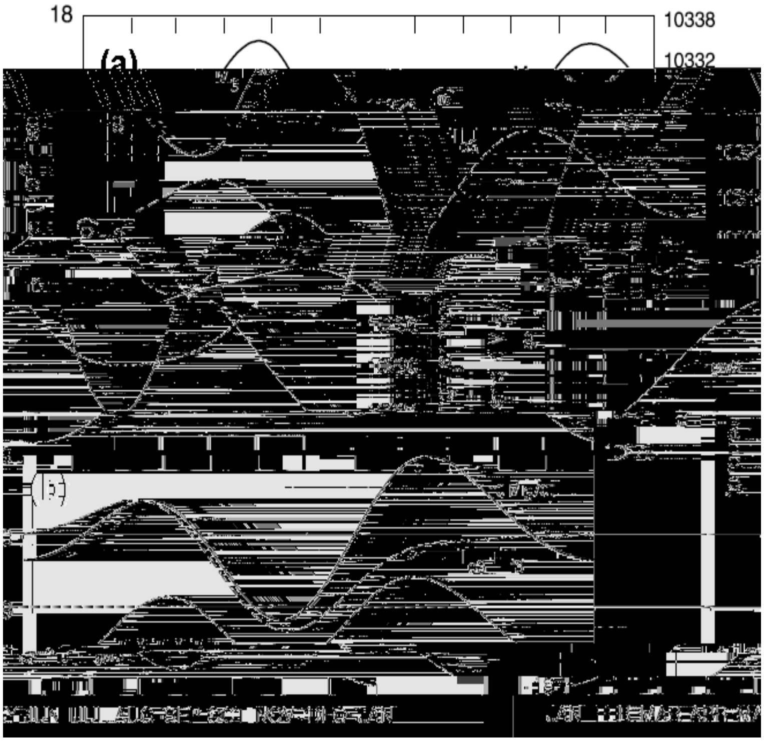

Figure 4.1: (a) All Torques and Angular Momentum - note the different scales (b) Angular Momentum tendency and summation of the torques. Figure adapted from Egger et al. (2007)

shown in figure 4.2. The power spectrum is the energy per unit time of a signal for a (user specified) range of frequencies. It allows us to see processes occuring on a given timescale.

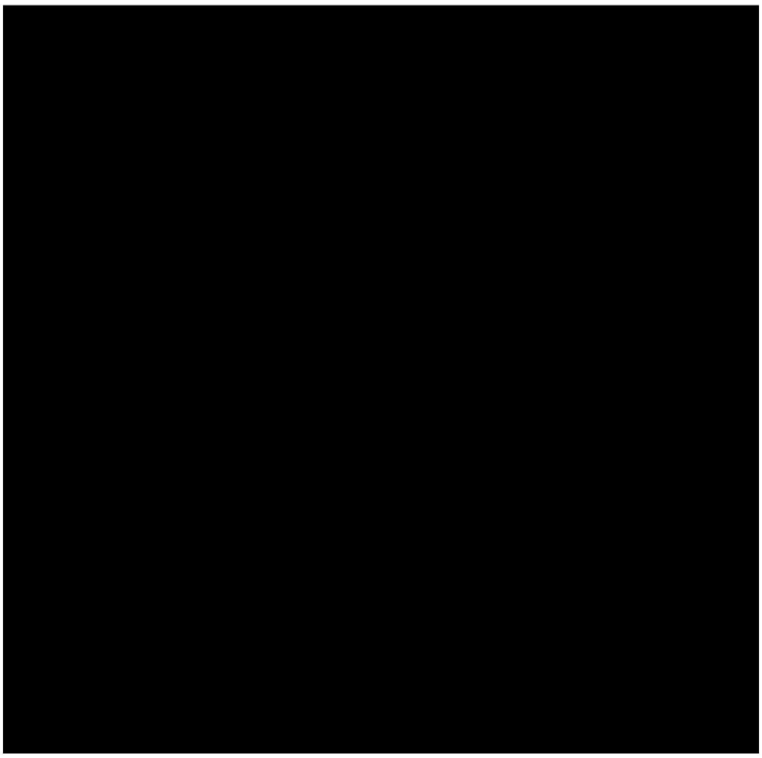

mountain and friction torque to the total torque depends on the timescale. Weickmann et al. (1997), further point to Swinbank (1985) who showed on synoptic scales that the mountain torque is much larger than the friction torque, and Madden and Speth (1995) who showed that this dominance continues out to at least 20-day fluctuations. However, within the timescale of interest to Weickmann et al. (1997), the two contribute about equally to the global torque, while in the zonal budget the friction torque is larger.

In this project we look at a reanalysis dataset and 3 climate models. We take data climate model data from the World Climate Research Programme's (WCRP's) Coupled Model Intercomparison Project phase 3 (CMIP3) multi-model dataset, described an "unprecedented collection of recent model output". The WCRP CMIP3 Multi-Model Database serves the serve IPCC's Working Group 1 (who focuses on the physical climate system - the atmosphere, land surface, ocean and sea ice). Information on the comprehensive specifications of the models is given at:
http : //www−pcmdi.llnl.gov/ipcc/model_documentation/ipcc_model_documentation.php

c c n

The NOAA Twentieth Century Reanalysis Version 2 Observation Dataset is produced by gular momentum on the climate models so need not concern ourselves with their vertical layers, and the gravity wave stress is not given in any of the models in the WCRP CMIP3

n

c

Many of the discrepancies in the angular momentum budget are very large and our choice of calculation does not require heavily compex schemes because we are not studying minute variations, however, in particular the mountain torque due to its derivative term requires special attention. We list here, only how we have chosen to calculate - a discussion of the considerations needed to be taken into account and the di□erent ways to calculate these terms is given in Appendix 1.

An n

Angular momentum can be written as

$$M = M_\Omega + M_r = \frac{R^4\Omega}{g}\int_{10}^{1000}\int_{\lambda=0}^{2\pi}\int_{\theta=-\pi/2}^{\pi/2} p_{sfc}\cos^3\theta d\theta d\lambda + \frac{R^3}{g}\int_{10}^{1000}\int_{\lambda=0}^{2\pi}\int_{\theta=-\pi/2}^{\pi/2} u\cos^2\theta d\theta d\lambda dp \tag{6.1}$$

as seen in Madden and Speth (1995). The limit 10hPa of the pressure integral is due to the fact that this is the roof limit for our, and many other, models. Ideally we would like to integrate over the whole of the atmosphere, however this is a reasonable approximation.

We take the approximation

$$M \approx \frac{R^4\Omega}{g} {}_{i} {}_{j} p^{i,j}_{sfc}\cos^3\theta_j \Delta \quad + d$$

itself.

It is important to be aware of potential potholes when working with velocities given on pressure levels. Consider a hill on which the surface pressure at three grid points lying on a line of constant latitiude is 990hPa, 987hPa, and 981hPa.

Velocity in the datasets is given on pressure levels of 1000hPa, 950 hPa, 900hPa, and so on (though not necessarily always decreasing by 50 hPa). If we were to try to integrate over the full volume of the atmosphere (1000hPa to 10 hPa) because the pressure at the surface at the three points is 990hPa, 987hPa, and 981hPa, between 990hPa and 1000hPa,

-0.230.234986(c)]TJ 987hPa and 1000hPa, or eda the friction stress is simply the value of friction stress directly from the model itself, and not from a forecast model that has processed the direct output.

For mountain torque we take

$$T_M = R^2 \int_{-\pi/2}^{\pi/2} Y_M \cos\theta d\theta \approx R^2 \sum_j^M Y_{M,j} \cos\theta_j \Delta\theta_j \tag{6.4}$$

where

$$Y_M = -\int_0^{2\pi} p \frac{\partial h}{\partial \lambda} d\lambda \approx \sum_i^N p_i \sum_{k=-K}^{k=K} b_k h_{i+k} = \sum_i^N \sum_{k=-K}^{k=K} p_i b_k h_{i+k} \tag{6.5}$$

and where we take the sixth ordered centered difference scheme as given by Weickmann and Huang (2008), shown in the table below

Table 6.1: 6th Order Centered Scheme b_k coefficients

k	-3	-2	-1	0	1	2	3
b_k	-1/60	3/20	-3/4	0	3/4	-3/20	1/60

On the NOAA Reanalysis datset the mountain torque was calculated by the pressure given by the dataset.

We take the approximation

$$T_G = R^3 \int_{\lambda=0}^{2\pi} \int_{\theta=-\pi/2}^{\pi/2} \tau_G \cos^2\theta d\theta d\lambda \approx R^3 \sum_i^N \sum_j^M \tau_G \cos^2 \Delta\theta_j \Delta\theta_i \tag{6.6}$$

for gravity wave torque. With the gravity wave stress τ_G taken from the forecast model.

We approximate the angular momentum tendency by

$$\left(\frac{dM}{dt}\right)_n \approx \frac{M_{n+1} - M_{n-1}}{2\Delta t_n} \tag{6.7}$$

The results from the NOAA Reanalysis Observation Dataset and the Climate Models show many commonalities with previous investigations whilst also having some interesting differences. However, the differences, which naturally occur between datasets, should not hold us back from saying that the agreement between our results calculated here and other papers over specific details gives us confidence that our results are correct. Such examples of this (which we shall discuss) are the range of values seen from our calculations and the range of values seen in previous investigations, the yearly average time series of angular momentum and the latitudinal friction profiles.

There are three points to take into account for reading the graphs

1. Sometimes we write ‘AM’ instead of Angular Momentum on the axes of the graphs when writing Angular Momentum would be too large to fit on the graph or would clutter the axes.

2. We also take the average yearly time series (as done in Egger et al. (2007), shown here as figure 4.1). The x-axis ranges from 1-12, where 1 is January and 12 December.

3. Lastly, in the latitudinal profiles that we plot a negative value of latitude corresponds to the degrees south of the equator, whilst a positive latitude corresponds to degrees north of the equator.

We first consider the time averages of the angular momentum and all the torques on the reanalysis dataset, then the latitudinal profiles of all the torques in the reanalysis, and then we consider the latitudinal profiles of all the torques in the climate models.

AA n y

A AA n y

We can see in the annual average plot of angular momentum that the annual maximums and minimums of angular momentum occur in the winter and summer, repectively, as they should do. We can clearly see that the angular momentum shows very close agreement in shape, and the basic underlying physics, with Egger et al. (2007). The angular momentum is larger than seen in other papers however, e.g. Madden and Speth (1995), and assuming superrotation (which is the idea that a planet's atmosphere rotates separately from, and faster than, the solid planet itself, and is taken here as a very crude approximation so that we can derive an approximate average speed of the whole atmosphere relative to the surface), the atmosphere has an a fairly small average velocity u_0, of $u_0 \sim 5ms^{-1}$ over 1961-1990, compared to Egger et al. (2007) that have $u_0 \sim 7ms^{-1}$, because of a smaller relative angular momentum in the NOAA reanalysis observation dataset (and thus the mass part of the angular momentum is quite large).

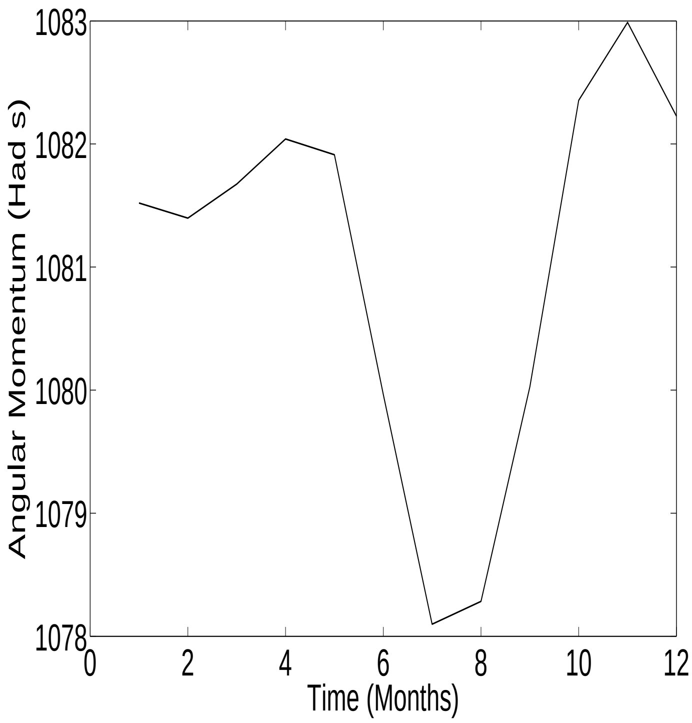

Figure 7.1: Year Average of the Reanalysis Dataset's Angular Momentum over 1961-1990

The 30 year average mountain torque shows many features that we would expect, and shows general agreement with Egger et al. (2007). We note that the minimum in the

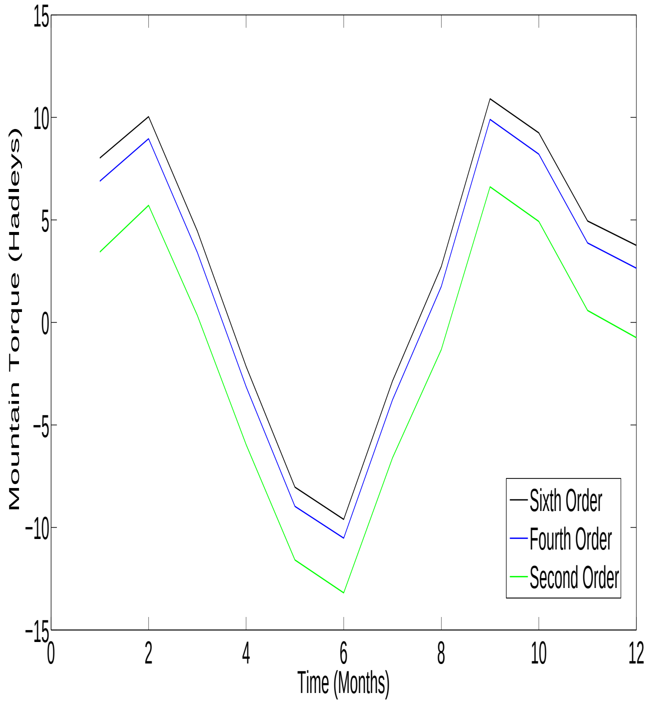

Figure 7.2: Year Average of the Reanalysis Dataset's Mountain Torque using three different centered schemes over 1961-1990

reanalysis observation dataset is about twice the size as that of Egger et al. (2007), and the reanalysis has a larger february peak than Egger et al. (2007). This means that at the time of minimum mountain torque we can expect more high pressure systems on the west side of the most important mountain ranges (contributing a steep negative gradient to the angular momentum tendency). The average value of the mountain torque over 1961-1990 is 2.8 Had - compare Huang et al. (1997) with 2.5 Had, and Egger et al. (2007) with -5 to -3 Had, indeed as noticed by Egger et al. (2007) the time mean value of mountain torque is highly uncertain. We calculated the mountain torque with three finite difference schemes, discussed in great detail in appendix 2, and we can see that, in line with previous research on the effect of the schemes conducted by Weickmann and Huang (2008), the lower the order scheme used, the more negative the value of mountain torque. Indeed, we see here a lower order causes a negative shift over all values of the mountain torque by a constant. The fact that the fourth order mountain torque is considerably closer to the sixth order scheme shows the rapid convergence to the true solution as the order used is increased that Weickmann and Huang (2008) speak of (indeed the difference between the sixth order scheme and higher order schemes would be negligible). Indeed, for the total torque investigations we took the most accurate value of mountain torque (sixth order).

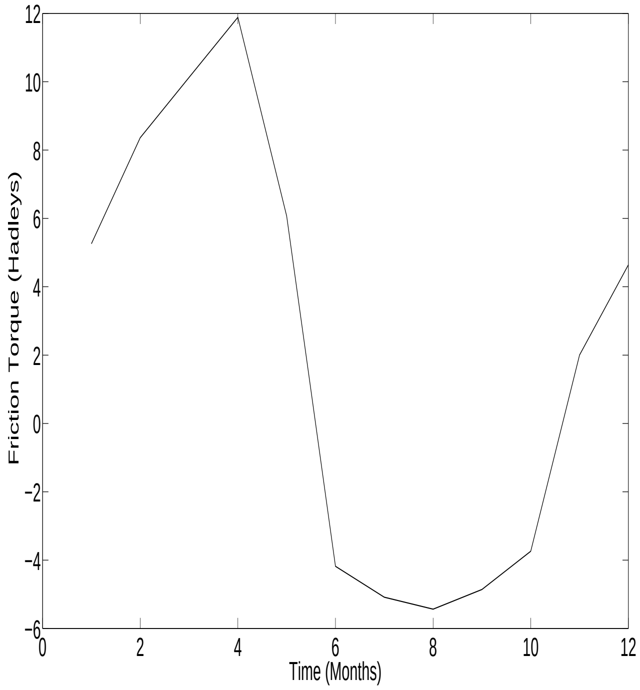

Figure 7.3: Year Average of the Reanalysis Dataset's Friction Torque over 1961-1990

Again the 30 year Friction Torque average shows us the same ge

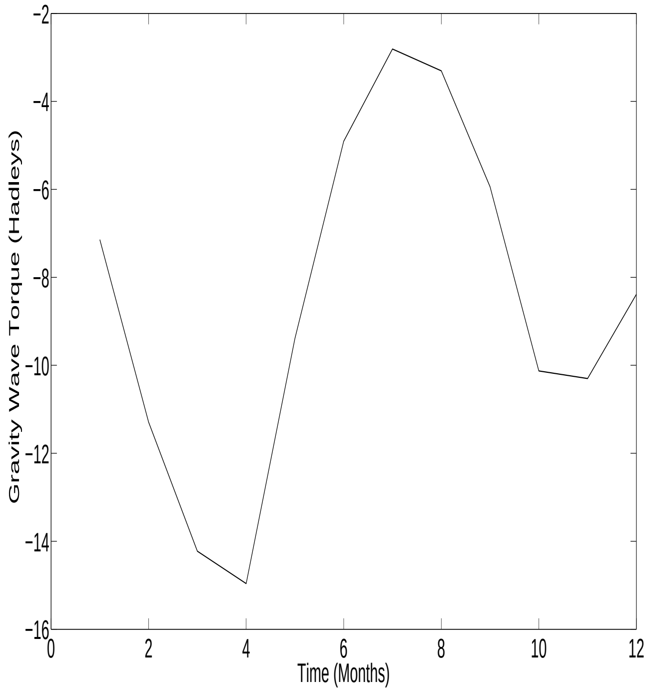

Figure 7.4: Year Average of the Reanalysis Dataset's Gravity Wave Torque

et al. (2007) who had -7.6 Had). The gravity wave torque graph, however, is significantly different to that of Egger et al. (2007). It has a very large winter rise, whilst in Egger et al. (2007) the gravity wave torque actually decreases during the winter months.

There is a rise in the gravity wave torque when the mountain torque is at its most active in removing angular momentum from the atmosphere, and the gravity wave torque appears like a mirror image of the mountain torque but delayed by one month so that when mountain torque increases/decreases the gravity wave torque decreases/increases.

We noticed another possible physical link with the gravity wave torque and the mountain torque. Whilst attempting to understand why the NOAA reanalysis gravity wave part of the mountain torque it would be peculiar for the gravity wave torque to precede the mountain torque in such a fashion.

to angular momentum tendency by roughly an addition by a constant. However, despite this problem, the average total torque is -3.8 Had ($-8.8 + 2.8 + 2.2$) (the closer to zero the better due to the requirement of total torque being zero over long periods of time as discussed in section 2.5), and indeed the fact that sometimes the total torque exceeds the seasonal cycle, and that during the northern hemisphere summer months there is much

the torques. Therefore we see conflict between what is happening, and what should be happening. Even if the dataset were to have decreasing torqu

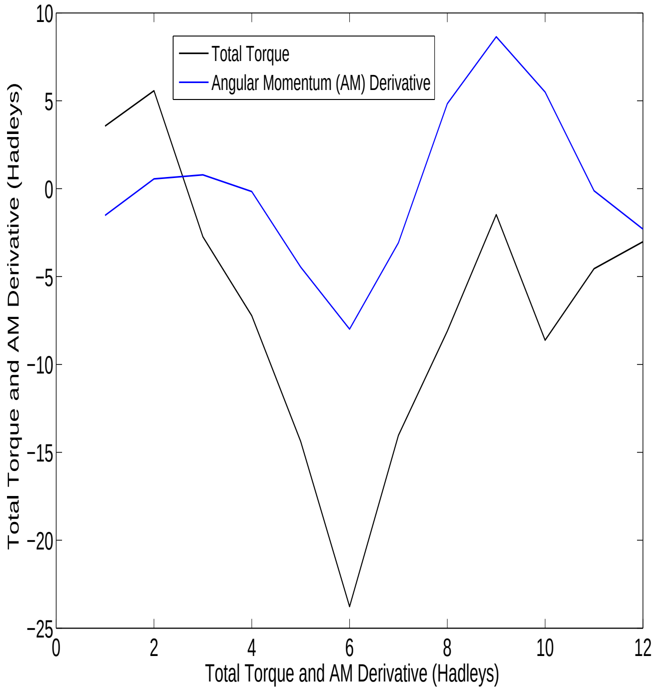

Figure 7.9: Yearly Average Angular Momentum Tendency and Total Torque for 1976-1990

L n n y n

The latitudinal profiles calculated allow us to see the (average monthly) contribution to the torque at each latitude over two decades: 1890-1899 and 1990-1999, giving us extra insight into the processes involved. They allow us to see that whether the torques we have seen in the timeseries not only have the right value when summed up over the globe, but whether the datasets' processes are physically correct and generate torques where they should. Taking profiles for two decades also tells us about their dependence on the resolution network required to produce accurate torques.

The mountain torque profile shows good agreement with the profile of Madden and Speth (1995), shown in figure 3.3, in size and shape, with the exception of a sharp peak which is the largest value appearing in the graph, yet is non-existent in Madden and Speth's investigation - we do not know of the cause of this, and whether the NOAA reanalysis is more accurate, or the dataset Madden and Speth analysed is more accurate. We see the presence of the Andes in the southern hemisphere removing angular momentum from the atmosphere, and likewise the himalayas and rocky mountains doing the same in the northern hemisphere. The mountain torque profiles over the two different decades are very similar, suggesting little dependence of the mountain torque on the resolution

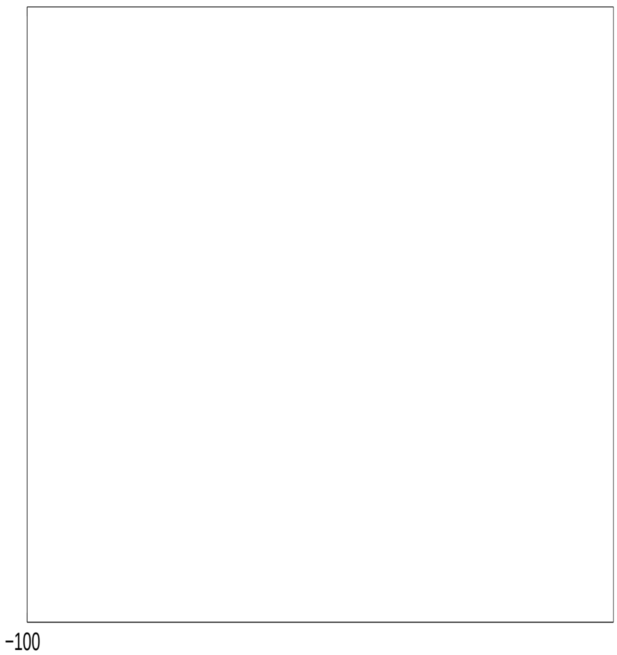
−100

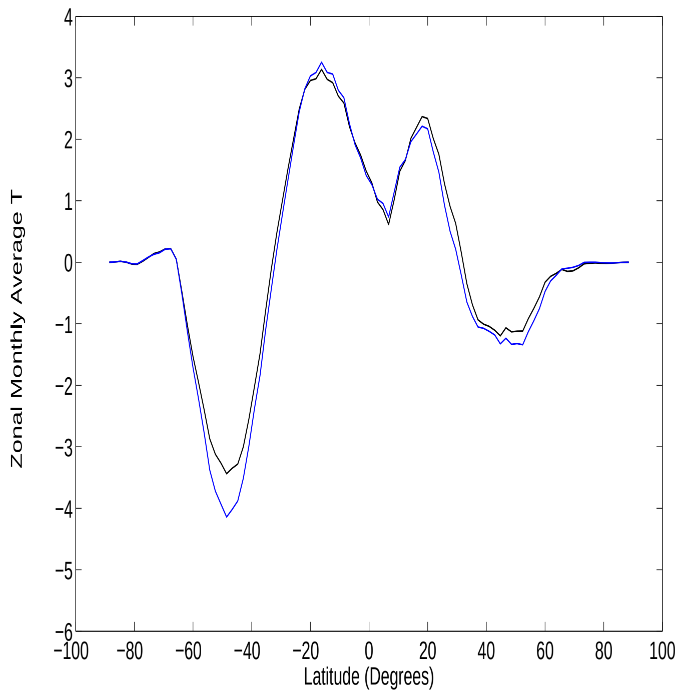

4
3
2
1
0
-1
-2
-3
-4
-5
-6
Zonal Monthly Average T
-100
-80
-60
-40
-20
0
20
40
60
80
100
Latitude (Degrees)

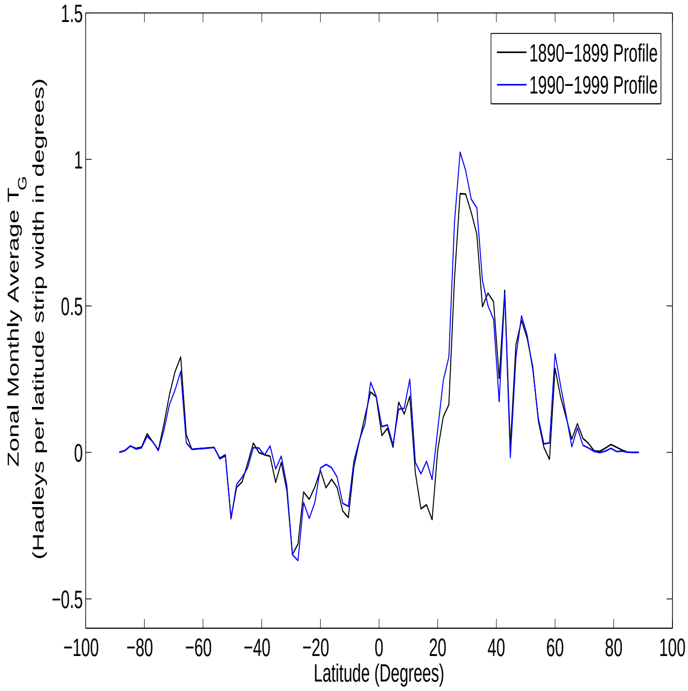

Figure 7.12: Monthly Average Reanalysis Dataset Latitudinal Gravity Wave Torque Profiles for 1890-1899 and 1990-1999

tudinal profile and the summer/autumn latitudinal profile in the following graph.

We see that the values of friction torque in the northern hemisphere equatorial regions are larger during the northern hemisphere winter/spring period than the yearly average or summer/autumn values in the same region. However, this should happen, as the winds throughout the northern hemisphere will be stronger during the northern hemisphere winter as shown in Peixoto and Oort (2007) (also recall our discussion of the increased northern hemisphere jet streams during the northern hemisphere winter in section 3.2, for example). Theret)4.034M297.44.034M297.44.034M297.44 LaLang 9377Ωmn lin .fan37561473(u)0.32898(

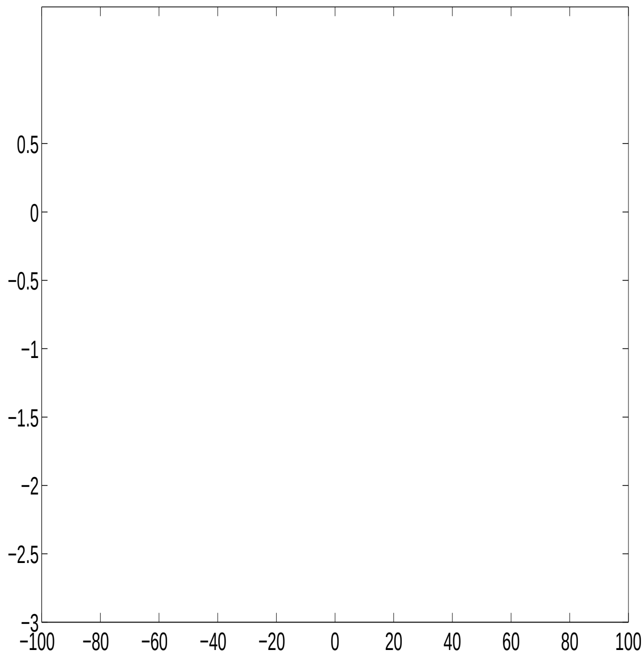
0.5
0
−0.5
−1
−1.5
−2
−2.5
−3
−100 −80 −60 −40 −20 0 20 40 60 80 100

The difference in the HadCM3 mountain torque profile over the two decades is very little suggesting little change in the pressure systems.

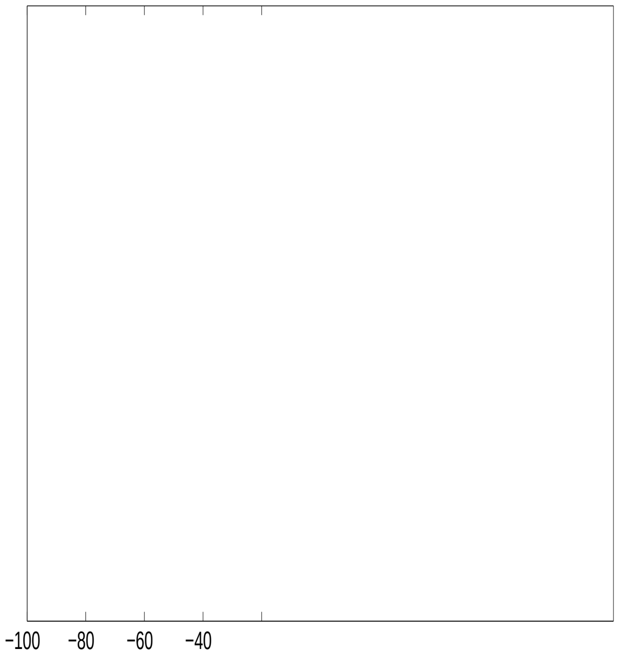

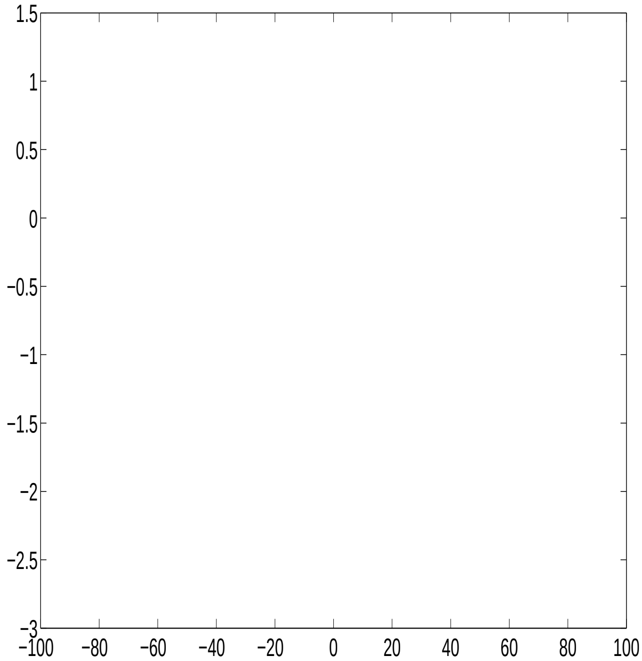

1.5
1
0.5
0
−0.5
−1
−1.5
−2
−2.5
−3
−100
−80
−60
−40
−20
0
20
40
60
80
100

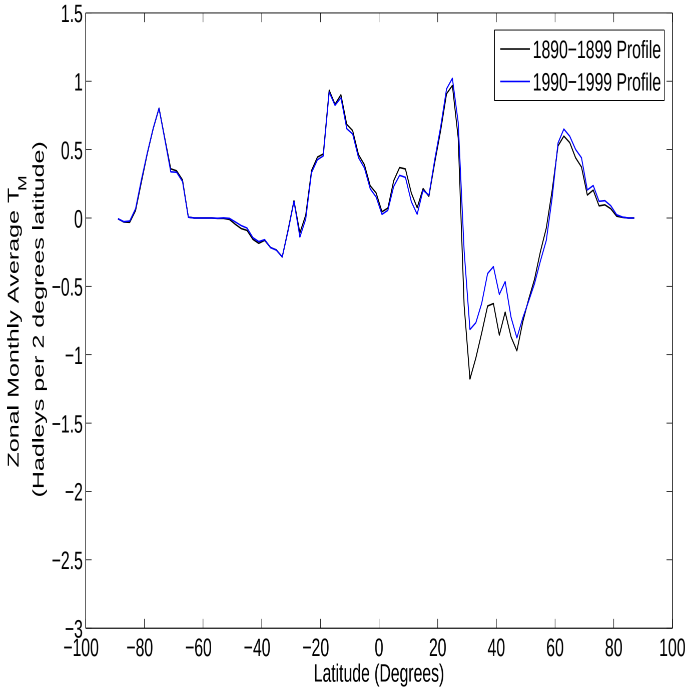

1890−1899 Profile
1990−1999 Profile
Zonal Monthly Average T_M
(Hadleys per 2 degrees latitude)
Latitude (Degrees)
1.5
1
0.5
0
−0.5
−1
−1.5
−2
−2.5
−3
−100
−80
−60
−40
−20
0
20
40
60
80
100

network can give the same latitudinal torque profiles as the observation network of today.

The climate models do show some promising features in their latitudinal profiles of the torques. Little change over time in the torques, and hence pressure systems, wind strengths and patterns, and so on, suggest consistency in the models with little serious model drift. However we see a clear difference in the HadCM3 model's mountain torque profile, and that of all others in this, and other, research. Further where this model repeats this pattern over both decades suggests that it is not just a passing anomaly, but a good reflection of the internal model physics. The mountain torque and friction torque of the NOAA GFDL CM2.0 climate model, were invariant over time, suggesting no visible drift. The mountain and friction torque profiles were almost symmetric about the equator suggesting that the atmosphere, as simulated in the model, is in a circulation pattern that is symmetric about the equator.

Whilst no datasets had identical latitudinal friction profiles, perhaps the most interesting difference in the friction profiles was between the Hadley Centre HadCM3 and HadGEM1 models - with the values in one model being twice the size of the other. We found this particularly interesting because the models are made by the same institute and are likely to have been constructed in a similar manner. We noted that the differences in sizes is most likely to be attributable to the wind speeds simulated in the models, and that HadGEM1 seems to have weaker surface winds than any climate model or observation dataset in this investigation. Also assuming reasonable angular momentum budget conservation in the models the difference in flux of angular momentum into the equatorial regions would have large scale applications for the atmospheric circulation the models.

Due to the lack of conservation of angular momentum, one recommendation from this dissertation is to investigate the causes of the erroneous torque values during the northern hemisphere winter in the reanalysis observation dataset. The idea of identifying the cause of such time dependent anomalies in the torques directly calls for the use of covariance analysis of the angular momentum and torques. This would allow us to glean the time dependent contributions and activity between the four variables (angular momentum, mountain, friction and gravity wave torque) that are associated with the atmospheric angular momentum budget.

Essentially the time covariances of the terms measure of how much two variables change together over time.

We take these ideas from Egger and Hoinka (2002) who sought to understand the time

3. That they satisfy both the conservation of angular momentum equation, equation (2.29), and they satisfy equation (8.3), i.e. the size of the torques and angular momentum, and the duration of torque and angular momentum events (and thus weather events) are the same.

tant work is being done on these models such as contribution of results to the next IPCC report. Specifically projects are being conducted to test the responses of climate models to volcanic eruptions in the research project “Stratospheric Particle Injection for Climate Engineering” (see the Stratospheric Particle Injection for Climate Engineering (SPICE) Project Website: http://gow.epsrc.ac.uk/ViewGrant.aspx?GrantRef=EP/I01473X/1).

In their paper, Shaw and Sheperd (2007), note that subject to radiative peturbation in the middle atmosphere the climate model response can be trustworthy or not. With angular momentum conservation and a range of gravity wave parameterizations the response of the climate models tested to this radiative peturbation is robust to changes such as the model lid height. However, when angular momentum is not conserved, due to the formulation or implementation of the gravity wave torque parameterization, there is a “non-negligible” spurious response from the imposed middle atmosphere radiative peturbation when the climate model lid height is changed. Further work into testing the conservation of angular momentum with the new raised lid models and investigations into their gravity wave torque parameterizations could be investigated as to whether this spurious response will occur in the model, contributing unreliable results to the project.

***

With knowledge of angular momentum theory and the code for calculating angular

A n n

The relationship between the spherical unit vectors $\mathbf{e}_\lambda$, $\mathbf{e}_\theta$ and $\mathbf{e}_r$ and the unit vectors in which we express angular momentum, taken from Egger et al. (2007), is shown below

$$\mathbf{e}_\lambda = -\mathbf{i}_1 \sin\lambda + \mathbf{i}\;\ \cos\lambda \tag{9.1}$$

$$\mathbf{e}_\theta = -\mathbf{i}_1 \cos\lambda \sin\theta - \mathbf{i}\;\ \sin\lambda \sin\theta + \mathbf{i}_3 \cos\theta \tag{9.2}$$

$$\mathbf{e}_r = \mathbf{i}_1 \cos\lambda \cos\theta + \mathbf{i}\;\ \sin\lambda \cos\theta + \mathbf{i}_3 \sin\theta \tag{9.3}$$

A n c n n

There is significantly more than just a choice of numerical approximation when choosing how to compute the angular momentum and torques because the choice of what to use to calculate the torques and angular momentum has a physical meaning.

Although it does not change our analysis, it should be noted that we do not strictly test equation (2.29) for all time, but the time averaged version

$$\frac{\partial \overline{M}}{\partial t} = \overline{T_F} + \overline{T_G} + \overline{T_M} \tag{10.1}$$

over a discrete set of values.

Recall the time average over a (time) interval $[0, \tau]$ of a variable A as

$$\overline{A} \equiv \frac{1}{\tau}\int_0^{\tau} A dt \tag{10.2}$$

In analysing the global angular momentum balance in reanalyses observation datasets and climate models it is essential we have a good numerical scheme for the computation of mountain torque because of its derivative term, as has been discussed by Weickmann and Huang (2008).

Mountain torque has been calculated by taking height and surface pressure in a fourier series at each latitude as done by Madden and Speth (1995) on a spectral model. Spectral models are a different type of model that represent the climatic variables over the globe without using grid points, however we shall not go into more detail on these models here. However, using this type of model the fourier series for the height was then differentiated with respect to λ

Then for

$$X_i = -p_i \left(\frac{\partial h}{\partial \lambda}\right)_i \tag{10.8}$$

they study six finite difference schemes

$$\left(\frac{\partial h}{\partial \lambda}\right)_i = \frac{1}{\Delta\lambda} \sum_{k=-K}^{k=K}$$

vector of surface pressure and Q is the matrix of coefficients resulting from the b_i chosen in the finite difference scheme).

Thus they look at

$$Y_{M,2} - Y_{M,1} = p^T Qh + h^T Qp \quad (10.11)$$

which can be written as

$$Y_{M,2} - y_{M,1} = h^T (Q + Q^T) p \quad (10.12)$$

and, Weickmann and Huang (2008) note that this is zero if $Q = -Q^T$, i.e. Q is antisymmetric. An encouraging find is that this is true for all centered difference schemes, whilst they note that the non-centered schemes do not satisfy this property.

y

We may take the values of the gravity wave stress from the model directly, or from the forecast values, in much the same way we did for friction stress.

Gravity Wave Torque has been studied much less over history, B

y

Johns, T. C. 2003. Anthropogenic climate change for 1860 to 2100 simulated with the HadCM3 model under updated emissions scenarios. Climate Dynamics 20:583612.

V. Lucarini: "Validation of Climate Models". This is a contributed article (pages 1053-1057) in: Ed. G. Philander, 2008. Encyclopedia of Global Warming and Climate Change. SAGE (Thousand Oaks, USA).

Madden, R.A, Speth. P., 1995. Estimates of Atmospheric Angular Momentum, Friction and Mountain Torques during 1987-1988. Journal of the Atmospheric Sciences, 52 (21), 3681-3694.

Meehl, G. A., Covey, C., Delworth, T., Latif, M., McAvaney, B., Mitchell, J.F.B., Stouffer, R.J., Taylor, K.E., 2007. The WCRP CMIP3 multi-model dataset: A new era in climate change research. Bulletin of the American Meteorological Society, 88, 1383-1394.

Oort, A., 1989. Angular Momentum in the Atmosphere-Ocean-Solid Earth System, from Gridded Global Datasets, Monthly Weather Review, 136, 4005-4009.

Weickmann, K.M., Sardeshmukh, P.D. 1994. The atmospheric angular momentum cycle associated with a Madden-Julian oscillation. Journal of the Atmospheric Sciences, vol.51, no.21, p. 3194-208

White, M., 1949. The Role of Mountains in the Angular-Momentum Balance of the Atmosphere. Journal of Meteorology, 6, 353-355.

Whitaker, J.S., G.P.Compo, X. Wei, and T.M. Hamill 2004: Rea